mls-2 and *vab-3* control glia development, *hlh-17*/Olig expression and glia-dependent neurite extension in *C. elegans*

Satoshi Yoshimura[1], John I. Murray[2], Yun Lu[1], Robert H. Waterston[2,3] and Shai Shaham[1,*]

Glia are essential components of nervous systems. However, genetic programs promoting glia development and regulating glia-neuron interactions have not been extensively explored. Here we describe transcriptional programs required for development and function of the *C. elegans* cephalic sheath (CEPsh) glia. We demonstrate ventral- and dorsal-restricted roles for the *mls-2*/Nkx/Hmx and *vab-3*/Pax6/Pax7 genes, respectively, in CEPsh glia differentiation and expression of the genes *hlh-17*/Olig and *ptr-10*/Patched-related. Using *mls-2* and *vab-3* mutants, as well as CEPsh glia-ablated animals, we show that CEPsh glia are important for sensory dendrite extension, axon guidance/branching within the nerve ring, and nerve ring assembly. We demonstrate that UNC-6/Netrin, expressed in ventral CEPsh glia, mediates glia-dependent axon guidance. Our results suggest possible similarities between CEPsh glia development and oligodendrocyte development in vertebrates, and demonstrate that *C. elegans* provides a unique environment for studying glial functions in vivo.

KEY WORDS: *C. elegans*, Glia, *hlh-17*, *mls-2*, Oligodendrocytes, *vab-3*

INTRODUCTION

Glia, the major cellular components of vertebrate nervous systems, play integral roles in nervous system development and function. For example, glia promote neuronal survival (Hosoya et al., 1995; Jones et al., 1995; Meyer-Franke et al., 1995) and generate directional cues for developing neurons and neurites (Edmondson et al., 1988; Fishell and Hatten, 1991; Serafini et al., 1996; Kidd et al., 1999; Noctor et al., 2001). Glia often ensheath neurons, and recent studies have addressed how oligodendrocytes, the myelinating glia of the vertebrate CNS, are generated (Briscoe et al., 2000; Jessell, 2000). Oligodendrocytes arise from discrete domains in ventral and dorsal regions of the developing spinal cord. Ventrally, the homeodomain transcription factors Nkx6.1/2 and Pax6 (Sun et al., 1998) are required for expression of the basic helix-loop-helix (bHLH) transcription factor Olig2 (Liu et al., 2003; Novitch et al., 2001; Vallstedt et al., 2001). Olig2, together with Olig1, controls neuroepithelial cell commitment to the oligodendrocyte lineage (Lu et al., 2000; Zhou et al., 2000). Genes promoting dorsal expression of Olig2 are unknown, but might include Pax7 (Cai et al., 2005; Fogarty et al., 2005; Vallstedt et al., 2005).

Despite burgeoning interest in glia and their functions, technical challenges in understanding their effects on neuronal activity and development remain. Importantly, because of their neurotrophic functions, glia manipulation often leads to neuronal death, preventing the study of glial contributions to other neuronal activities. Identification of systems in which glia are not required for neuronal viability could allow unprecedented access to understanding glial influences on neurons.

The *Caenorhabditis elegans* hermaphrodite contains 50 glial cells associated with sensory organs of the animal (Heiman and Shaham, 2007; Shaham, 2006). Although the morphology and anatomy of these glia have been characterized (Ward et al., 1975; White et al., 1986), their functions are not well understood. Of these glia, four cephalic sheath (CEPsh) glia, which associate with CEP dopaminergic sensory dendrites (Fig. 1A), also send sheet-like processes that envelop the nerve ring, a neuropil generally viewed as the animal's brain (Fig. 1B,C). Roles for CEPsh glia in synaptogenesis have been suggested (Colón-Ramos et al., 2007).

Here we show that *C. elegans* CEPsh glia are not required for neuronal survival, enabling in vivo studies of their influences on neuronal development. We show that ventral and dorsal CEPsh glia develop through molecularly distinguishable pathways regulated by the Nkx/Hmx-related gene *mls-2* and the *Pax6/7*-related gene *vab-3*, respectively. These genes regulate glial expression of the *C. elegans* Olig1/2-related gene *hlh-17*. Using *mls-2* mutants, *vab-3* mutants, and cell ablations, we describe roles for CEPsh glia in dendrite extension and axon branching/guidance, showing that these latter functions are mediated by UNC-6/Netrin.

Our results suggest that *C. elegans* might provide a novel setting for exploring in vivo aspects of glial cell development and glia-neuron interactions.

MATERIALS AND METHODS

Strains

Strains were handled using standard methods (Brenner, 1974) and were maintained at 20°C, unless otherwise indicated. The wild-type strain used was *C. elegans* var. Bristol (N2). Strain and integrated transgene references are as follows. LGI: *nsIs105* (*hlh-17*::GFP); LGIV: *nsIs136* (*ptr-10*::myrRFP), *hlh-17* [*ns204*, *ok487* (McMiller and Johnson, 2005)], *hlh-31* (*ns217*), *hlh-32* (*ns223*), *sDf23* (Ferguson and Horvitz, 1985); LGV: *oyIs17* (*gcy-8*::GFP) (Satterlee et al., 2001), *oyIs44* (*odr-1*::RFP) (Lanjuin et al., 2003), *oyIs51* (T08G3.3::RFP) (Lanjuin et al., 2006), *nsIs145* (*ttx-1*::RFP), *otIs45* (*unc-119*::GFP) (Altun-Gultekin et al., 2001); LGX: *mls-2* [*ns156*, *ns158*, *ns159*, *cc615* (Jiang et al., 2005)]; *vab-3* [*ns157*, *e648* (Hodgkin, 1983), *e1796* (Hedgecock et al., 1987), *ju468*, *sy281*, *k109*, *k143* (Cinar and Chisholm, 2004), *bx23* (Baird et al., 1991)]; *nsIs108* (*ptr-10*::myrRFP).

[1]The Rockefeller University, Laboratory of Developmental Genetics, 1230 York Avenue, New York, NY 10065, USA. [2]Department of Genome Sciences, University of Washington, Seattle, WA 98195, USA. [3]Division of Basic Sciences, Fred Hutchinson Cancer Research Center, Seattle, WA 98105, USA.

*Author for correspondence (e-mail: shaham@rockefeller.edu)

egIs1 (*dat-1*::GFP) (Nass et al., 2005), *nIs60* (*vab-3* promoter::GFP, gift from Andrew Chisholm), *zuIs178* (*his-72*::H3.3-GFP) (Ooi et al., 2006) and *ruIs32* (*pie-1*::H2B-GFP) (Praitis et al., 2001) insertions are unmapped. *nT1 qIs51* IV; V (Siegfried et al., 2004) was used as a balancer for *hlh-17* (*ok487*) and *sDf23*.

The following extrachromosomal arrays were used: *nsEx646* [*hlh-17*::myrGFP + *lin15*(+)], *nsEx725* [*hlh-31* promoter::RFP + *lin15*(+)], *nsEx729* [*hlh-32* promoter::RFP + *lin15*(+)], *nsEx1420* [C39E6 + *rol-6* (*su1006*)], *nsEx1419* [*mls-2* promoter::*mls-2* + *rol-6* (*su1006*)], *nsEx1404* [F14F3 + *rol-6* (*su1006*)], *nsEx1463* [heat-shock promoter::*mls-2* + *rol-6* (*su1006*)], *nsEx1464* [heat-shock promoter::*vab-3* + *rol-6* (*su1006*)], *nsEx1577* [*mls-2* promoter::*vab-3*::*mls-2*::*mls-2* 3′ UTR + *rol-6* (*su1006*)], *nsEx1717* [C39E6 + *nhr-38*::GFP + *elt-2*::GFP].

Mutagenesis and mapping

hlh-17::GFP animals were mutagenized with 30 mM ethyl methanesulfonate (Sulston and Hodgkin, 1988) and plated on 9-cm NGM agar plates. F1 adults were individually plated on 1600 plates and F2 progeny were screened for CEPsh glia defects. Mutants were mapped by crossing to strain CB4856, followed by isolation of homozygous mutant animals and SNP genotyping (Wicks et al., 2001).

Plasmid constructs

hlh-31 promoter::RFP

We amplified by PCR a 1.5 kb DNA fragment from cosmid F38C2 containing 1.2 kb sequences upstream of the *hlh-31* first ATG as well as the coding sequence for the first 32 amino acids. The amplicon was ligated to the RFP gene digested with *Sph*I and *Bam*HI. No expression was detected for *hlh-31*.

hlh-32 promoter::RFP

We amplified a 3 kb DNA fragment upstream of the *hlh-32* ATG from the YAC Y105C5. The amplicon was ligated to the RFP gene digested with *Sph*I and *Bam*HI. The *hlh-32* transgene was expressed in two unidentified neurons in the head.

hlh-17::GFP

To define an *hlh-17* promoter element, we sequenced *hlh-17* cDNAs and identified some containing the SL1 trans-spliced leader (Krause and Hirsh, 1987), enabling identification of a putative ATG. To generate the reporter we amplified a 2.7 kb DNA fragment from cosmid F38C2 containing 1.9 kb of sequences upstream of the *hlh-17* ATG and sequences encoding the first 58 amino acids. The 1.9 kb promoter fragment included a 96 bp segment immediately upstream of the ATG. This segment was not present in a transgene previously described (Fig. 1E) (McMiller and Johnson, 2005). The amplicon was ligated to pPD95.69 (Miller et al., 1999) digested with *Sph*I and *Bam*HI.

hlh-17::myrGFP

We amplified a 4 kb DNA fragment from cosmid F38C2 containing sequences upstream of the *hlh-17* ATG. The amplicon was ligated to the myrGFP gene (Adler et al., 2006) digested with *Sph*I and *Bam*HI.

ptr-10::myrRFP

We amplified a 300 bp DNA fragment from cosmid F55F8 containing genomic sequence upstream of the *ptr-10* ATG. The amplicon was ligated to the myrRFP gene (Adler et al., 2006) digested with *Sph*I and *Xma*I.

mls-2 promoter::GFP::*mls-2*::*mls-2* 3′ UTR

See Jiang et al. (Jiang et al., 2005).

mls-2 promoter::*vab-3*::*mls-2*::*mls-2* 3′ UTR

vab-3 isoform A cDNA was digested with *Sal*I and ligated into the *mls-2* promoter::GFP::*mls-2*::*mls-2* 3′ UTR construct digested with *Sal*I, replacing GFP with *vab-3*.

Heat-shock promoter::*mls-2*/*vab-3*

mls-2/*vab-3* isoform A cDNAs were digested with *Age*I and *Eco*RI and ligated into the same sites of vector pPD95.75 (Miller et al., 1999). The heat-shock promoter was amplified from vector pPD49.78 (Fire et al., 1990), digested with *Sph*I and *Bam*HI, and ligated into the same sites as the cDNA vectors.

8.3 kb C39E6 subclone

We amplified an 8.3 kb DNA fragment from cosmid C39E6 containing 5.5 kb of sequences upstream of the *mls-2* ATG, the *mls-2* coding sequence, and 300 bp downstream of the *mls-2* stop codon. The amplicon was digested with *Pst*I and *Eco*RI and ligated into the same sites of pPD95.75.

Transgenic strains

Germline transformations were carried out as published (Mello and Fire, 1995). *hlh-17*::GFP (50 ng/μl) and *ttx-1*::RFP (3 ng/μl) were injected into N2 animals. *ptr-10*::myrRFP (50 ng/μl) was injected into *lin-15*(*n765*) animals with plasmid pJM23 (20 ng/μl) containing *lin-15* (Huang et al., 1994). Extrachromosomal transgenes were integrated using 4,5′,8-trimethylpsoralen followed by insertion homozygote identification (Yandell et al., 1994).

For *mls-2* rescue experiments, cosmid C39E6 and its 8.3 kb subclone were injected into *mls-2*(*ns156*) animals (1 ng/μl). For *vab-3* rescue experiments, cosmid F14F3 or a 24 kb *Asc*I-*Pme*I subclone were injected into *vab-3*(*ns157*) animals (1 ng/μl). The *mls-2* promoter::*vab-3*::*mls-2*::*mls-2* 3′ UTR construct was injected into N2 animals with plasmid pRF4 (40 ng/μl) containing the dominant marker *rol-6* (*su1006*) (Mello et al., 1991) (20 ng/μl). Other reporter constructs were injected into animals at 30-50 ng/μl with either pRF4, pJM23 or *elt-2*::GFP (Fukushige et al., 1998) as transformation markers (30-40 ng/μl).

Ablations

Strains used for ablation contained either *hlh-17*::GFP or *ptr-10*::myrRFP together with a neuronal marker to facilitate scoring of CEPsh glia fate and axonal defects. In some cases, ablated strains contained *unc-119*::GFP (Maduro and Pilgrim, 1995). Precursor cells of CEPsh glia were ablated in embryos at the 250-300 minute stage in a drop of S-basal buffer on 5% agar pads using a micropoint laser set up (Bargmann and Avery, 1995). These cells were identified by following the cell division patterns of embryos (Sulston et al., 1983). Ablations were scored as successful if CEPsh glia were absent 2 days later.

Isolation of deletion mutants

Deletion alleles were isolated using published methods (Jansen et al., 1997; Hess et al., 2004). The following primer pairs (5′ to 3′) were used for screening: *hlh-17*: poison primer, GCATGACTTAAACGAGGCACT-TGACG; outer primers, ATGGGGTCCCTGGGGACTC and CCGATTTCCGCTTCAACTGGGAG; inner primers, TCCCTGG-GGACTCTCCTCG and CGATTTTTGCTGCTAATGGGCAACAC. *hlh-31*: poison primer, GCATGACTTAAACGAGGCACTTGACG; outer primers, CAGTCCGGATGGAATGAACAAAAGGG and CTACATG-GTCGCTTGATGGCTTCAC; inner primers, TTGCAGCCAACTCAA-AGTTGGGTC and GGGAGACCAATACACTGAGCTCC. *hlh-32*: poison primer, GCATGACTTAAACGAGGCACTTGACG; outer primers, GCCTCTGGTAGTCTACGGC and CTAATCTCCTTCGGATGGTGT-TGACACGG; inner primers, GCTTCCGTTTTTGGGAAACAAGAG and CTTAGCTCTTCGATTGCTTTTGCCTG.

cDNA isolation

cDNAs for *hlh-17*, *hlh-31*, *hlh-32*, *mls-2* and *vab-3* were isolated by amplification using PCR of a plasmid-based cDNA library (Schumacher et al., 2005) using primers within the vector and within the genes.

Mosaic analyses

C39E6, *nhr-38*::GFP and *elt-2*::GFP were co-injected at 1 ng/μl, 50 ng/μl and 20 ng/μl, respectively, into a strain of genotype *nsIs105* (*hlh-17*::GFP); *nsIs145* (*ttx-1*::RFP); *mls-2*(*ns156*). Animals harboring the extrachromosomal array were selected using *elt-2*::GFP expression under a fluorescence dissecting microscope, mounted for observation on a compound microscope in M9 medium, and assessed for appearance of *hlh-17*::GFP and *nhr-38*::GFP expression in the ventral CEPsh glia and AFD neurons, respectively. Similar studies were performed for *vab-3* mosaic studies, except that the *vab-3* cosmid, F14F3, was injected together with *ptr-10*::myrRFP into *vab-3*(*ns157*) mutants carrying an integrated *hlh-17*::GFP reporter, and animals lacking *hlh-17*::GFP expression in subsets of CEPsh glia were examined.

For the *unc-6* mosaic studies, we used an *elt-2*::GFP reporter (Fukushige et al., 1998) to follow transgenic animals.

Microscopy

Animals were examined by epifluorescence using either a fluorescence dissecting microscope (Leica), an Axioplan II compound microscope (Zeiss), or a spinning disc confocal microscope (Zeiss) equipped with a Perkin-Elmer UltraView spinning disk confocal head. For the compound microscope, images were captured using an AxioCam CCD camera (Zeiss) and analyzed using the Axiovision software (Zeiss). For the spinning disk confocal microscope, images were captured using an EMCCD (C9100-12) gain camera (Hamamatsu) and analyzed using MetaMorph software (UIC). Electron microscopy was carried out on serial sections as previously described (Perens and Shaham, 2005).

Heat-shock studies

Heat-shock constructs were injected at 20 ng/µl with pRF4 (40 ng/µl) as the transformation marker. Animals were placed at 34°C for 30 minutes, allowed to recover at 20°C, and scored for induction of reporters 60-150 minutes later.

Southern hybridizations

Preparation of genomic DNA, agarose gel electrophoresis and Southern blotting were performed using standard techniques (Ausubel et al., 1989). Probes were prepared from *hlh-17* cDNA by PCR.

Lineage analysis

Lineage tracing was performed essentially as described by Murray et al. (Murray et al., 2006). Three-dimensional time-lapse image series were collected for wild-type (*n*=2), *mls-2*(*ns156*) (*n*=4) and *vab-3*(*ns157*) (*n*=4) embryos carrying a nuclear-localized *his-72*::H3.3-GFP reporter using a Zeiss LSM510 confocal microscope. We used StarryNite (Bao et al., 2006) to automatically trace the lineage from the images, and AceTree (Boyle et al., 2006) to identify and edit errors in the StarryNite annotations. Lineages were followed through the 350-cell stage and the CEPsh-producing lineages (ABarpa, ABplpaa, ABprpaa) selectively traced through the birth of the CEPsh glia. Because StarryNite makes significantly more errors at and beyond the 350-cell stage than it does at earlier stages, we followed each cell by eye in each lineage throughout its lifespan and corrected all errors. Tree displays and 3D projections were generated in AceTree.

RESULTS

hlh-17/Olig-related and ptr-10/Patched-related are expressed in CEPsh and other glia

To investigate the roles of CEPsh glia in *C. elegans* nervous system development, we sought to identify reporters that would allow us to visualize these cells. We used two approaches. First, we surmised that *C. elegans* genes similar to known vertebrate regulators of glial cell fate might be expressed in *C. elegans* glia. In vertebrates, *Olig2* encodes a bHLH transcription factor involved in oligodendrocyte and motoneuron development (Lu et al., 2002; Lu et al., 2000; Takebayashi et al., 2002; Zhou and Anderson, 2002; Zhou et al., 2000). Comparison of the Olig2 protein sequence to predicted *C. elegans* proteins using BLAST (Altschul et al., 1990) revealed three genes, *hlh-17*, *hlh-31* and *hlh-32*, situated within a 140 kb region of chromosome IV, encoding proteins exhibiting similarity to the bHLH domain of Olig2 (71, 59 and 71% identity, respectively; Fig. 1D; see Fig. S5A in the supplementary material). To determine whether these genes are expressed in glia, we generated animals carrying transgenes in which promoter regions of each gene were placed upstream of either GFP or the monomeric/multimeric *Discosoma* Red reporter genes (RFP/DsRed; see Fig. S5E in the supplementary material). Although neither the *hlh-31* nor *hlh-32* reporter transgene was expressed in glia (see Materials and methods), a transgene, containing 1.9 kb of sequence upstream of the *hlh-17* translation start site and 0.8 kb downstream of the start site fused to GFP, was expressed strongly in CEPsh glia at all developmental stages (Fig. 1F) (McMiller and Johnson, 2005) and in some motoneurons of the ventral cord in larvae (see Fig. S1 in the

supplementary material). This expression pattern is reminiscent of *Olig2* expression in oligodendrocyte and motoneuron lineages (Lu et al., 2000; Zhou et al., 2000).

As a second approach to identify CEPsh glia reporters, we turned to our previous studies demonstrating that DAF-6 protein, which is related to the Hedgehog receptor Patched, is expressed in glia of amphid and phasmid sensory organs (Perens and Shaham, 2005). *C. elegans* encodes 24 Patched-related proteins (Kuwabara and Labouesse, 2002; Kuwabara et al., 2000) and we hypothesized that some might be expressed in CEPsh glia. We found that a myristoylated RFP, under the control of a 300 bp *ptr-10* promoter fragment, was expressed in CEPsh glia (Fig. 1G,H) and in sheath and socket glia of inner and outer labial sensilla, and of the deirid (see Fig. S1G-L in the supplementary material).

CEPsh glia are important for CEP neuron dendrite extension

The availability of CEPsh glia reporters allowed us to explore the functions of these cells during nervous system development. For example, the association of CEPsh glial processes with CEP neuron dendritic processes (Fig. 1A) suggests that blocking CEPsh glia formation might result in CEP dendritic defects. To test this, we ablated direct precursors of CEPsh glia in animals carrying either *hlh-17*::GFP or *ptr-10*::myrRFP reporters using a laser microbeam, confirming ablations by the absence of reporter expression. Importantly, we never observed neuronal death following ablations: 205/206 operated animals examined in the studies described in this paper showed normal neuronal marker expression.

We found that 4/4 animals in which the ventral left CEPsh glia precursor, ABplpaaapap, was ablated, had shortened ventral left CEP neuron dendrites, as assessed by expression of the CEP neuron reporter *dat-1*::GFP (Nass et al., 2005). Similarly, 4/4 animals in which the dorsal left CEPsh glia precursor, ABarpaaaapp, was ablated, displayed shortened dorsal left CEP dendrites (Fig. 2), suggesting that CEPsh glia are important for CEP neuron dendrite extension.

CEPsh glia also control axon guidance and branching in the nerve ring

CEPsh glia also associate with the nerve ring and ventral ganglion (Fig. 1A-C). Thus, we surmised that eliminating CEPsh glia might, in addition to perturbing dendrite extension, affect nerve ring axon outgrowth [a similar hypothesis was proposed by Wadsworth et al. (Wadsworth et al., 1996)].

The axons of the AWC, AFD and ADF sensory neurons enter the nerve ring through the ventral ganglion (White et al., 1986). To assess the effects of CEPsh glia on the development of these axons, we ablated ventral CEPsh glia precursors in animals carrying the reporters *odr-1*::RFP [AWC (L'Etoile and Bargmann 2000)], *ttx-1*::DsRed [AFD (Satterlee et al., 2001)] or T08G3.3::RFP [ADF (Sagasti et al., 1999)]. Whereas the axon shapes and lengths of the three neurons are highly regular in wild-type animals, we observed multiple defects in these neurites in operated animals, ranging from a lack of ventrally directed processes to abnormal branching. Major defect classes are depicted in Fig. 3A-H. Defects were more pronounced for AWC and AFD axons than for ADF axons (Fig. 3I). Guidance and branching defects of these neurons were generally observed when ventral, but not dorsal, CEPsh glia precursors were ablated (Fig. 3I).

Taken together, these studies demonstrate that CEPsh glia play spatially restricted roles in axon guidance within the nerve ring. Importantly, these guidance roles appear to be neuron specific.
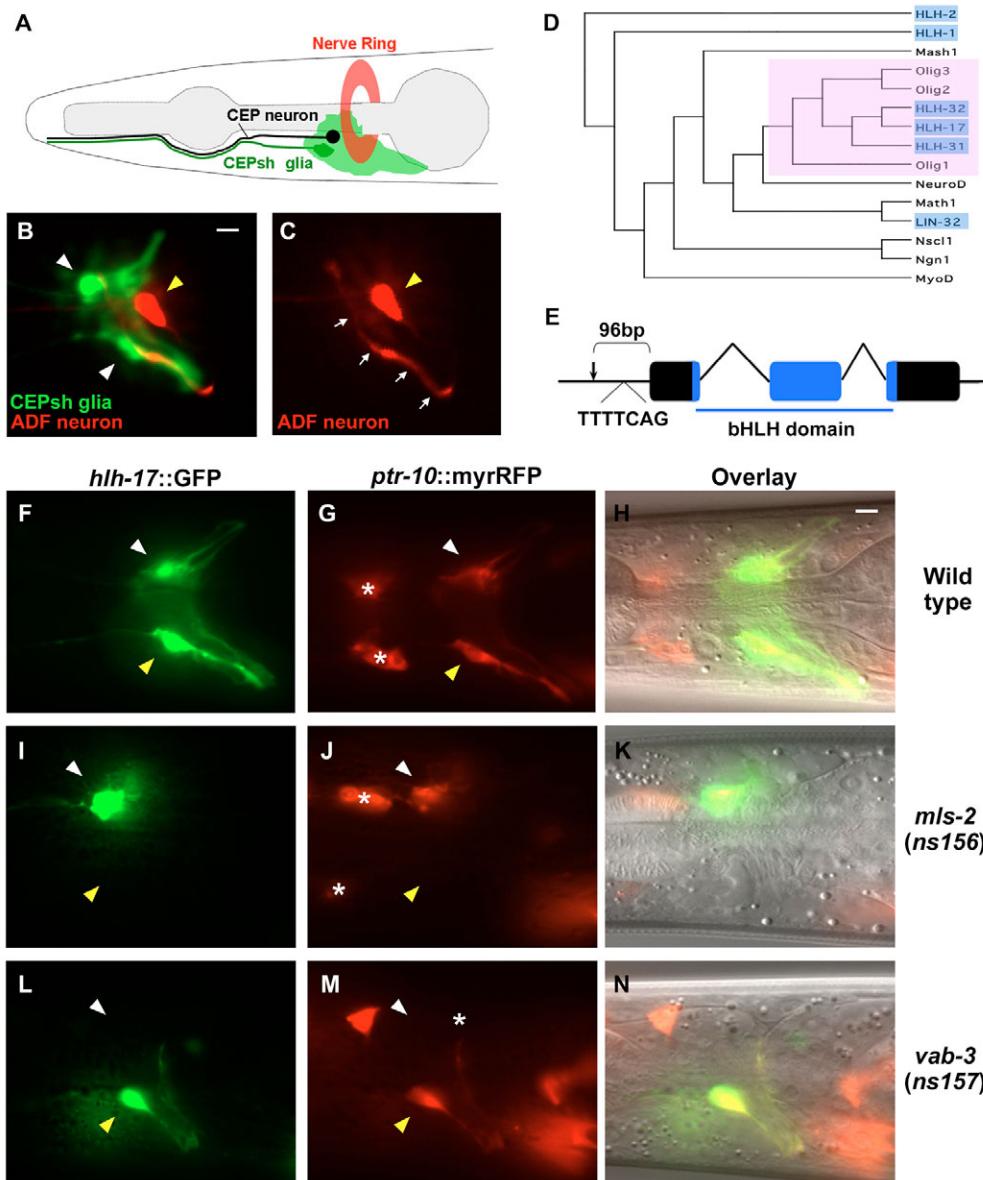
Fig. 1. *mls-2* and *vab-3* regulate the development of ventral and dorsal CEPsh glia, respectively. (**A**) The *C. elegans* head. In all figures, dorsal is up and anterior is left. Posterior regions of ventral CEPsh glia ensheath the ventral ganglion. (**B,C**) Fluorescence images of a wild-type adult expressing *hlh-17*::GFP in CEPsh glia (white arrowheads) and the T08G3.3::RFP ADF neuron reporter (yellow arrowheads). (**B**) Overlay. (**C**) ADF alone. White arrows, ADF axon. (**D**) Dendogram depicting similarity of HLH-17 to Olig and other human and *C. elegans* bHLH protein subfamilies. (**E**) *C. elegans hlh-17* gene structure. Boxes, exons; ∧-shaped lines, introns; arrow, position of a previously predicted translation start site different from that described here (see Materials and methods); TTTTCAG, trans-splicing site; the bHLH domain is in blue. (**F-N**) Fluorescence (F,G,I,J,L,M) and merged DIC/fluorescence (H,K,N) images of wild-type (F-H), *mls-2(ns156)* (I-K) and *vab-3(ns157)* (L-N) adults expressing *hlh-17*::GFP and *ptr-10*::myrRFP. White and yellow arrowheads indicate dorsal and ventral CEPsh glia, respectively. Asterisks indicate non-CEPsh glia. Scale bars: 5 μm.

One explanation for the differential effects of ventral CEPsh glia on different axons is that at certain points within the nerve ring and ventral ganglion, some axons are closer to ventral CEPsh glia processes than others. To determine whether such regions of the nerve ring exist, we examined previous electron microscopy (EM) reconstructions of the nerve ring (White et al., 1986). Indeed, axons of the AWC and AFD neurons are situated adjacent to CEPsh glia processes at two different locations along their lengths, on the outer surfaces of the nerve ring and ventral ganglion (see Fig. S2 in the supplementary material). By contrast, ADF axons are distal to CEPsh glia processes. These observations suggest that short-range signals from CEPsh glia to specific axons might determine axon guidance and branching decisions.

### UNC-6/Netrin mediates glia-dependent axon guidance

One possible axon guidance cue expressed by CEPsh glia is the *C. elegans* Netrin protein UNC-6, which is expressed in ventral but not dorsal CEPsh glia (Wadsworth et al., 1996). To determine whether UNC-6 mediates CEPsh glia-dependent axon guidance, we first examined the effects of a strong loss-of-function mutation in *unc-6(ev400)* on AWC axon guidance. Fifty-four of 102 animals displayed guidance defects in at least one of the two bilateral AWC axons, suggesting roles for *unc-6* in AWC axon guidance.

To determine in which cells *unc-6* functions for AWC axon guidance, we generated *unc-6(ev400)* animals containing an integrated AWC reporter and an unstable extrachromosomal array consisting of *hlh-17*::GFP and plasmid ΔpSM containing a rescuing *unc-6* gene (Colón-Ramos et al., 2007). Twenty-four out of 25 animals expressing *hlh-17*::GFP in ventral CEPsh glia had normal axon outgrowth. By contrast, 12/23 animals expressing *hlh-17*::GFP in dorsal but not ventral CEPsh glia had normal axon outgrowth, similar to animals lacking *unc-6*. These results, together with the *unc-6* expression pattern, strongly suggest that UNC-6 functions within ventral CEPsh glia to control AWC axon guidance.

CEPsh glia may control nerve ring assembly

During our ablation studies, we noticed that 17/91 animals in which ventral CEPsh glia were ablated arrested development in the L1 larval stage. L1 arrest was not observed in mock-ablated animals and
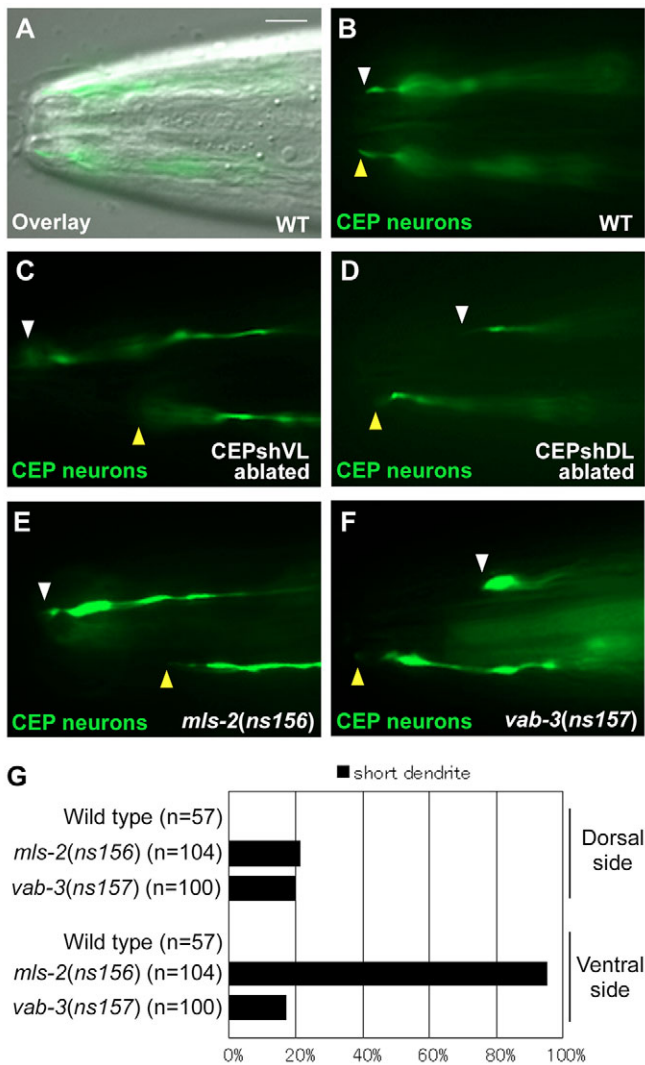
Fig. 2. CEPsh glia are required for CEP neuron dendrite extension. (**A**) Merged DIC/fluorescence and (**B**) fluorescence image of wild-type (WT) adult *C. elegans* expressing *dat-1*::GFP in CEP neurons. White and yellow arrowheads indicate dorsal and ventral left dendrite tips, respectively. (**C,D**) Fluorescence images of *dat-1*::GFP-expressing adult animals lacking either ventral (C) or dorsal (D) left CEPsh glia. (**E,F**) Fluorescence images of *mls-2(ns156)* (E) and *vab-3(ns157)* (F) adults, respectively, expressing *dat-1*::GFP. (**G**) Dendrite extension defects of strains of the indicated genotype. Scale bar: 5 μm.

was rarely seen when cells near the CEPsh precursors were ablated (1/26 ablated animals). AWC, AFD and ADF neurons in arrested larvae displayed severe defects in axon projections, suggesting global defects in nerve ring assembly. To examine the integrity of the nerve ring in ablated animals, we ablated ventral CEPsh glia precursors in animals carrying the *unc-119*::GFP pan-neuronal reporter. Six out of 30 animals examined exhibited L1 arrest, highly disorganized nerve rings and anteriorly displaced neuronal cell bodies (Fig. 3R-U). The incomplete penetrance of these defects might reflect functions of the remaining dorsal CEPsh cells, which could not be reliably ablated in animals operated ventrally, and/or neuron-intrinsic cues allowing self-assembly. The early onset of nerve ring defects suggests problems with assembly and not maintenance of the structure. Consistent with this notion, ablation

of all CEPsh glia in L1 animals does not affect nerve ring structure or axon guidance in adults (*n*=120; M. Katz, S.Y. and S.S., unpublished).

These results suggest that CEPsh glia might be important not only for the guidance and branching of specific axons within the nerve ring, but also for the assembly of the entire structure.

The development of ventral and dorsal CEPsh glia are molecularly distinguishable

To understand the molecular basis of CEPsh glia development, we sought to identify mutants with defects similar to those of CEPsh glia-ablated animals. We mutagenized animals carrying an integrated *hlh-17*::GFP reporter and scanned F2 progeny for alterations in reporter expression.

Four mutants we isolated form two complementation groups consisting of the three alleles *ns156*, *ns158*, *ns159*, and the single allele *ns157*, and had reciprocal effects on ventral and dorsal CEPsh glia development (Fig. 1F-N). As shown in Fig. 4, most *ns156* (as well as *ns158* and *ns159*) animals lacked expression of *hlh-17*::GFP and *ptr-10*::myrRFP in ventral CEPsh glia, whereas reporter expression was usually maintained in dorsal CEPsh glia. Reciprocally, most *ns157* animals lacked *hlh-17*::GFP and *ptr-10*::myrRFP expression in dorsal CEPsh glia, whereas nearly half expressed these reporters in ventral CEPsh glia. Expression of reporter genes in at least some cells other than the CEPsh glia was essentially unaffected in these mutants (data not shown). Although defects in reporter transgene expression could be found in all CEPsh glia, the dorsal/ventral bias in these defects demonstrates that despite morphological similarities, the development of dorsal and ventral CEPsh glia are molecularly distinguishable.

CEPsh glia are abnormal in *ns156* and *ns157* mutants

The absence of reporter transgene expression in *ns156* and *ns157* mutants could reflect defects in either CEPsh glia fate specification or generation. To distinguish between these possibilities, we used automated 4D lineage tracking (Bao et al., 2006) to follow cell divisions leading to CEPsh glia generation in *ns156* and *ns157* mutants. In 4/4 *ns156* and 4/4 *ns157* animals examined, all CEPsh glia were generated (see Fig. S3 in the supplementary material) and were properly positioned, with the exception of a single anteriorly displaced dorsal CEPsh cell in one *ns156* embryo. These results suggest that the *ns156* and *ns157* mutations do not block CEPsh glia generation and that CEPsh glia precursors are grossly normal. Thus, these mutations probably disrupt CEPsh glia terminal differentiation or fate specification.

To determine whether CEPsh glia features other than reporter expression were perturbed in these mutants, we used EM to examine whether CEPsh glia ensheathed the nerve ring and ventral ganglion leading into the nerve ring. In 2/2 *ns157* animals examined, ensheathment was observed (data not shown). However, in 2/2 *ns156* animals, ventral ensheathment was absent (see Fig. S4 in the supplementary material). Furthermore, ventral ganglia of both *ns156* mutants were disorganized, lacking characteristic bilateral symmetry (see Fig. S4 in the supplementary material). These results suggest that *ns156* disrupts CEPsh glia differentiation/specification more severely than *ns157*.

To further assess CEPsh glia defects in *ns156* and *ns157* mutants, we examined CEP dendrite extension in these animals. We found that CEP dendrites in these mutants are shorter than in wild-type animals (Fig. 2E,F), although the shortened dendrites still possessed cilia (Fig. 2E), as in CEPsh glia-ablated animals. Consistent with the
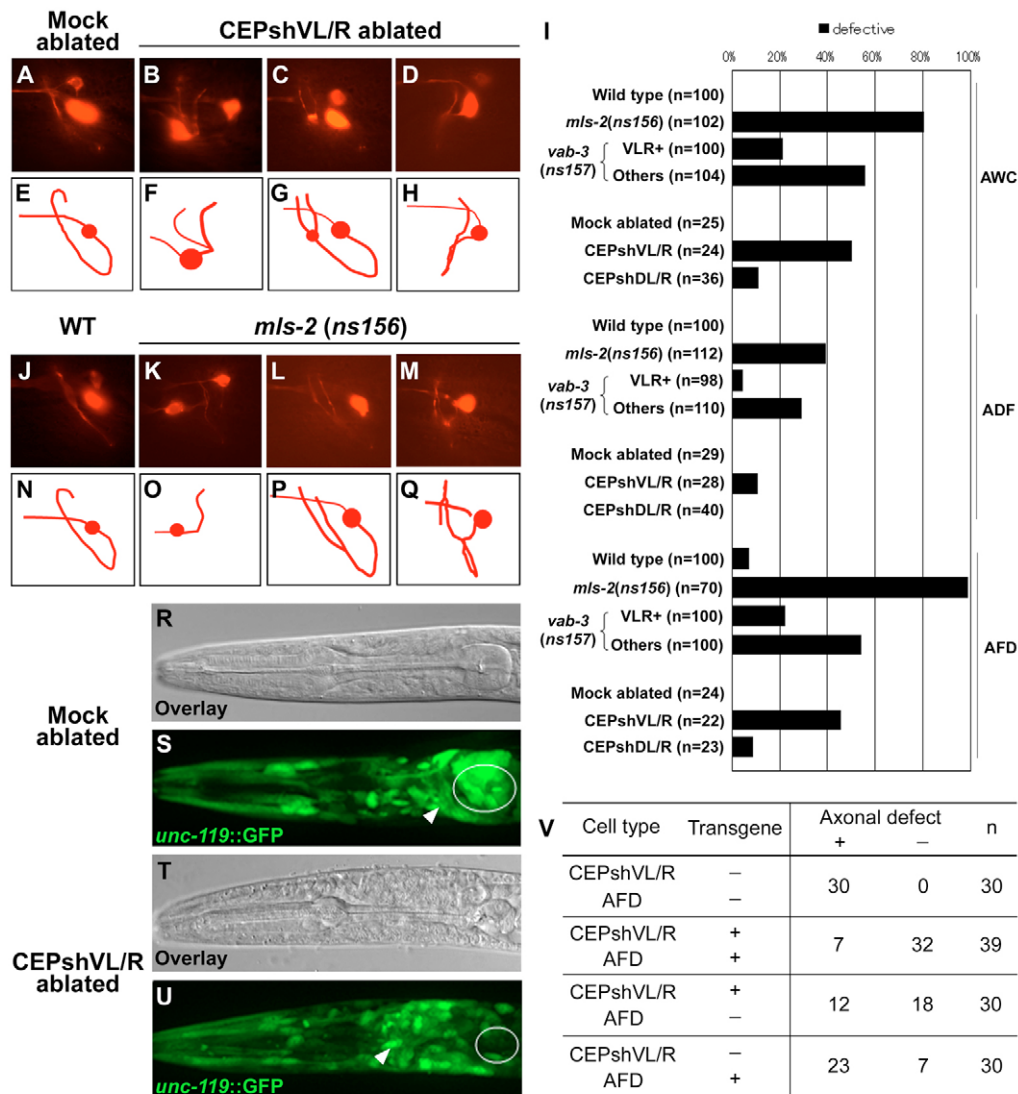
Fig. 3. CEPsh glia support axon guidance in the nerve ring. (**A-H**) AWC axonal defects of adult *C. elegans* lacking ventral left and right CEPsh glia. Fluorescence images (A-D) and corresponding schematics (E-H) of AWC neurons expressing *odr-1*::RFP. (A,E) Mock-ablated animal. (B-D,F-H) AWC defects frequently observed in operated animals. In all panels, the reporter is also expressed in AWB axons. (**J-Q**) AWC axon defects observed in *mls-2(ns156)* adults. Fluorescence images (J-M) and corresponding schematics (N-Q) of AWC neurons expressing *odr-1*::RFP. (J,N) Wild-type AWC axon. (K-M,O-Q) AWC defects of *mls-2(ns156)* adults. In J-M, reporter is also expressed in AWB neurons. Similar defects are seen in *vab-3(ns157)* mutants and in AFD neurons of *mls-2(ns156)* and *vab-3(ns157)* animals. (**I**) Histogram depicting AWC, ADF and AFD axonal defects in animals of indicated genotype or in which CEPsh glia were ablated. VL/R+, expressing *hlh-17*::GFP in ventral left and right CEPsh glia. Others, lacking *hlh-17*::GFP in one or both ventral CEPsh glia. *n*, number of animals. Some *mls-2(ns156)* mutants fail to express AWC reporters. We only scored animals in which robust expression was evident. (**R-U**) DIC (R,T) and fluorescence (S,U) images of wild-type L1 animal (R,S) and an L1 with ablated ventral left and right CEPsh glia (T,U) expressing *unc-119*::GFP. The posterior pharyngeal bulb is circled. Arrowhead, nerve ring. Note the abnormal positioning and shape of the nerve ring in the ablated animal. (**V**) Mosaic studies of *mls-2*. Axonal defect +, AFD axon defect; axonal defect −, no defect; *n*, number of animals; transgene +, transgene present; transgene −, transgene absent.

defects in *hlh-17* and *ptr-10* reporter expression, CEP dendritic defects in *ns156* mutants are mostly restricted to ventral dendrites (Fig. 2G). In *ns157* mutants, defects were seen in 20% and 17% of dendrites of dorsal and ventral CEP neurons, respectively (Fig. 2G), consistent with the EM studies suggesting that *ns157* mutants have subtler defects than *ns156* mutants (see Fig. S4 in the supplementary material).

We also examined *ns156* and *ns157* mutants for defects in AWC, AFD and ADF axon guidance. Defects were observed in both mutants (Fig. 3). Major *ns156* defects are depicted in Fig. 3J-Q, and are reminiscent of defects seen in glia-ablated mutants.

Similar abnormalities were seen in *ns157* animals. As in CEPsh glia-ablated animals, *ns156* and *ns157* mutants preferentially affect AWC and AFD axon guidance, and have weaker effects on ADF. It is of note that in *ns156* mutants, AFD, and perhaps AWC, guidance is more disrupted than in CEPsh glia-ablated animals (Fig. 3I), suggesting that some of the defects seen in these mutants might be due to abnormalities in cells other than CEPsh glia.

Finally, we also noted that 38% of *ns156* mutants examined (*n*=577) arrest as L1 larvae and display nerve ring assembly defects resembling those seen in CEPsh glia-ablated animals.
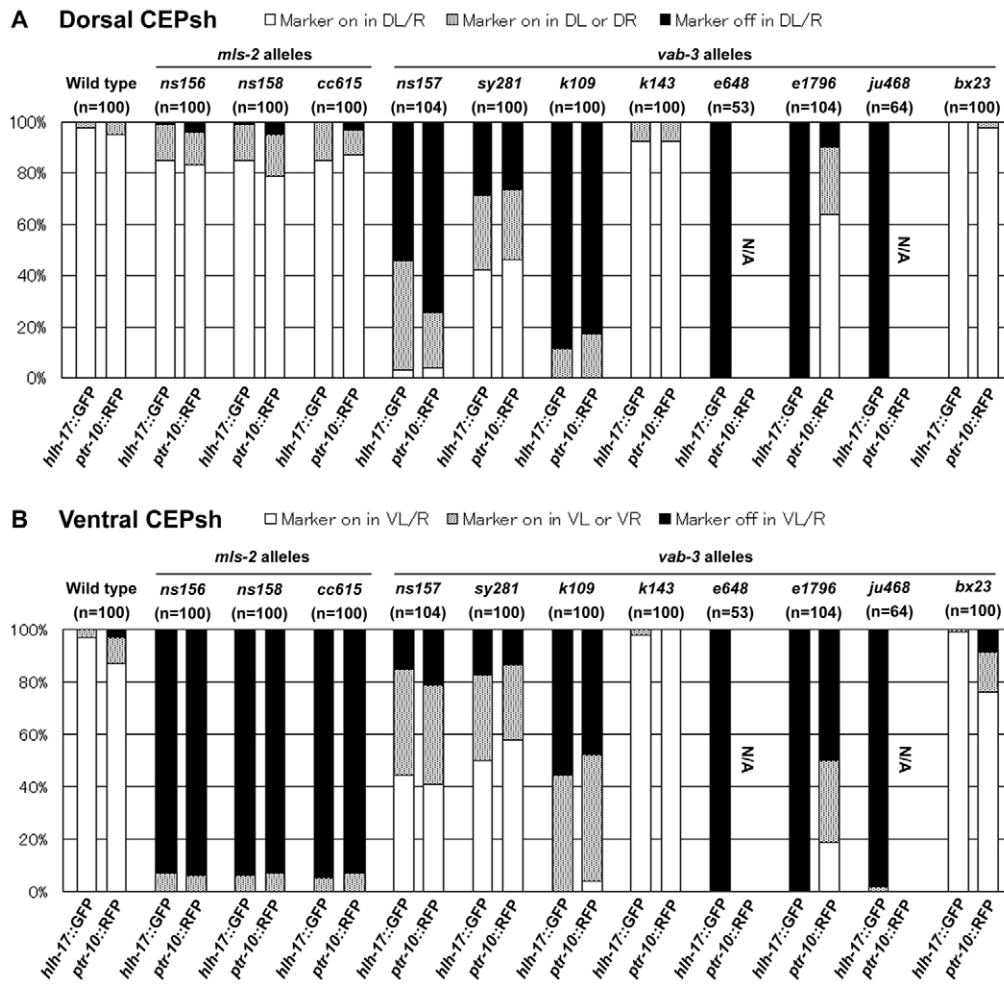
Fig. 4. *mls-2* and *vab-3* mutations affect CEPsh glia differentiation. Histograms of reporter expression in (**A**) dorsal and (**B**) ventral CEPsh glia of indicated mutants. Vertical axis, percentage of animals showing marker expression; *n*, number of animals examined. N/A, not applicable: in these animals, cells are mispositioned, making CEPsh glia identification difficult. VL/R and DL/R, ventral left/right and dorsal left/right CEPsh glia, respectively.

Taken together, the studies described above strongly support the notion that the *ns156* and *ns157* mutations affect genes important for CEPsh glia differentiation. Furthermore, these studies support the idea that CEPsh glia play key roles in regulating axon guidance, nerve ring assembly and CEP dendrite extension.

mls-2, an Nkx/Hmx-related gene, controls ventral CEPsh glia differentiation
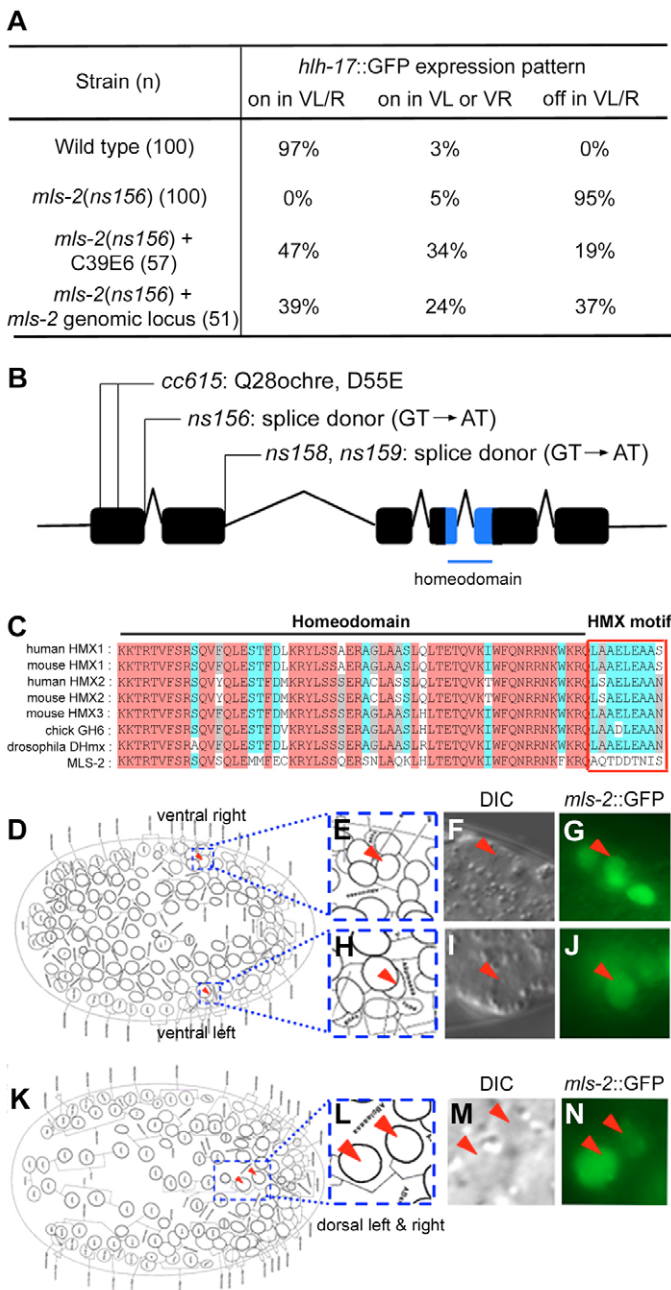
We used single nucleotide polymorphism (SNP) mapping and transformation rescue to demonstrate that the *ns156* mutation disrupts the gene *mls-2* (Fig. 5A). Molecular lesions in *mls-2* were identified in *ns156*, *ns158* and *ns159* mutants (Fig. 5B), and defects similar to those of *ns156* mutants were observed in animals carrying the previously reported *mls-2*(*cc615*) mutation (Jiang et al., 2005) (Fig. 4). *mls-2* encodes a protein with a homeodomain similar to those of HMX/Nkx5 transcriptional regulators, but lacks the HMX motif, [A/S]A[E/D]LEAA[N/S], located immediately downstream of HMX homeodomains (Fig. 5C) (Wang et al., 2000). Because Nkx proteins are closely related to HMX proteins, but lack the HMX motif, *mls-2* might be more appropriately classified as an Nkx superfamily member.

To determine where *mls-2* functions to regulate CEPsh glia differentiation, we generated animals carrying a rescuing transgene in which we inserted GFP upstream of *mls-2* coding regions in an 8.3 kb *mls-2* rescuing genomic fragment (see Fig. S5E in the supplementary material). We found that GFP::*mls-2* was expressed in nuclei of the precursor cells of the left and right ventral CEPsh glia, ABplpaaapap

and ABprpaaapap, respectively (Fig. 5D-J), and probably within CEPsh cells themselves (although the high density of cells in this region precluded reliable identification, and expression was extinguished postembryonically). GFP expression was also detected in the precursors of dorsal CEPsh glia (Fig. 5K-N), consistent with our observations that *mls-2* mutants weakly affect *hlh-17*::GFP and *ptr-10*::myrRFP expression in these glia (Fig. 4).

To further confirm that *mls-2* functions in the CEPsh glia lineage we performed a mosaic analysis aimed at defining the site of *mls-2* function in directing AFD axon guidance. We generated *mls-2* mutants carrying integrated *hlh-17*::GFP and *ttx-1*::DsRed reporters to label the CEPsh glia and AFD neurons, respectively. Into these mutants, we introduced the *mls-2* rescuing cosmid and the AFD-specific reporter, *nhr-38*::GFP, both on an unstable extrachromosomal array. Ventral *hlh-17*::GFP expression presumably indicated the array was present in ventral CEPsh glia (an assumption that gave the most parsimonious interpretation of the data in Fig. 3V). The presence of this array in AFD was scored by *nhr-38*::GFP expression. As shown in Fig. 3V, when the array was absent from both CEPsh glia and AFD neurons, all animals displayed axon defects. However, when the array was present in both AFD neurons and CEPsh glia, most animals had no axonal defects. The *ttx-1*::DsRed reporter had a weak (10%) effect on AFD axon guidance on its own. These results support the notion that the *ns156* axonal defects are caused by the *mls-2* lesion.

We then examined animals in which the array was present in one or the other cell type. We found that in 60% of animals in which the array was present in ventral CEPsh glia, but absent from AFD neurons, axon

A

Strain (n)	*hlh-17*::GFP expression pattern		
	on in VL/R	on in VL or VR	off in VL/R
Wild type (100)	97%	3%	0%
mls-2(ns156) (100)	0%	5%	95%
mls-2(ns156) + C39E6 (57)	47%	34%	19%
mls-2(ns156) + *mls-2* genomic locus (51)	39%	24%	37%

B

C

Fig. 5. *ns156* alters MLS-2, an Nkx/HMX-related homeodomain protein. (**A**) *mls-2(ns156)* rescue studies. Strains were scored as in Fig. 4. VL/R, ventral left/right CEPsh glia. *n*, number of animals. C39E6, *mls-2* cosmid. One representative line is shown for each construct. The *mls-2* genomic locus construct contains 8.3 kb surrounding and including the gene. (**B**) *C. elegans mls-2* gene structure. Boxes, exons; ∧-shaped lines, introns; the homeodomain is in blue. (**C**) Alignment of homeodomains and HMX motifs of MLS-2 and related proteins. Pink, identical in all; blue, identical in all but one or two proteins; gray, present in five proteins. (**D-J**) (D) Diagram of ventral nuclei positions in a 270-minute embryo [adapted with permission from Sulston et al. (Sulston et al., 1983)]. (E,H) Enlarged regions of D, (F,I) DIC and (G,J) fluorescence images of a ventral right (E-G) and left (H-J) CEPsh glial cell precursor (red arrowhead) in a 270-minute embryo expressing *mls-2*::GFP. (**K-N**) Same as D-G but showing dorsal left and right CEPsh glia precursors.

guidance was rescued. However, if the array was present only in AFD neurons, 23% of animals had wild-type axons, consistent with the idea that *mls-2* affects axon guidance non-autonomously and that *mls-2* activity resides within the CEPsh glia lineage.

vab-3, a *Pax6/7*-related gene, functions in CEPsh glia to regulate glia development

We used SNP mapping and transformation rescue (Materials and methods) to demonstrate that *ns157* disrupts the gene *vab-3* (Fig. 6A). *vab-3* is the *C. elegans* gene most similar to the vertebrate *Pax6* and *Pax7* genes; it encodes two DNA-binding domains – a Paired domain (PD) and a homeodomain (HD) – and generates three transcripts, A, B and C (Chisholm and Horvitz, 1995). We identified a missense mutation within the *vab-3* PD in *ns157* mutants, confirming identification of the gene (Fig. 6B).

To determine whether *vab-3* functions within CEPsh glia to regulate their differentiation, we performed a mosaic analysis. We introduced an extrachromosomal array containing the *vab-3* cosmid and *ptr-10*::myrRFP into *vab-3(ns157)* mutants carrying an integrated *hlh-17*::GFP reporter and searched for animals lacking *hlh-17*::GFP expression. We found a perfect correlation between *ptr-10*::myrRFP and *hlh-17*::GFP expression in dorsal CEPsh glia (Fig. 6D). Importantly, we never observed *ptr-10*::myrRFP expression in CEPsh cells lacking *hlh-17*::GFP (*n*=12), consistent with *vab-3* functioning within, or in cells closely related to, CEPsh glia to control differentiation.

To confirm the mosaic studies, we inserted a *vab-3* isoform A cDNA directly downstream of the 5.5 kb *mls-2* promoter in the *mls-2* rescuing genomic clone, and introduced this transgene into *vab-3(ns157)* mutants. The transgene exhibited weak but reproducible rescue of *hlh-17* and *ptr-10* reporter expression in dorsal CEPsh glia: 18/100 (18%) animals carrying the transgene expressed *hlh-17*::GFP in both dorsal left and right CEPsh glia, whereas only 3/104 (2.9%) animals without the transgene expressed *hlh-17*::GFP in these cells.

To further confirm that *vab-3* functions in the CEPsh lineage, we took advantage of the observation that *vab-3(ns157)* mutants show partially penetrant defects in *hlh-17*::GFP expression in ventral CEPsh cells (Fig. 4). As shown in Fig. 3I, AWC, AFD and ADF axon defects in *vab-3(ns157)* mutants were more severe if *hlh-17*::GFP expression was also disrupted in ventral CEPsh glia, consistent with the idea that *vab-3* functions in CEPsh glia and that CEPsh glia are required for axon morphogenesis.
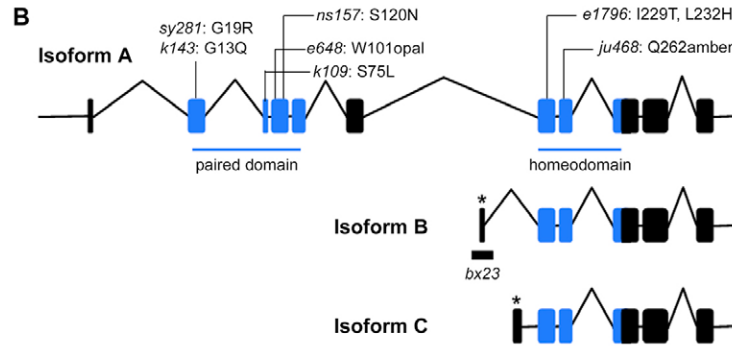
Different VAB-3 domains may regulate *hlh-17* and *ptr-10* expression in dorsal and ventral CEPsh glia

Although *vab-3(ns157)* mutants show a bias towards dorsal defects in reporter transgene expression, the molecular lesion in these animals may not abolish *vab-3* function and, thus, the phenotype of *vab-3(ns157)* animals might not represent the *vab-3*(null) phenotype. To test this, we examined CEPsh reporter transgene expression in animals homozygous for two *vab-3* alleles, *e648* and *ju468*, that eliminate most, if not all, activity of *vab-3* isoform A (Fig. 6B) (Chisholm and Horvitz, 1995; Cinar and Chisholm, 2004). We were unable to detect *hlh-17*::GFP expression in either dorsal or ventral CEPsh glia in these animals (Fig. 4), suggesting that *vab-3* is important for differentiation of all CEPsh glia, and that the weaker phenotype of *ns157* mutants is due to residual *vab-3* function.

The *vab-3(ns157)* lesion promotes defects preferentially in dorsal CEPsh glia. Interestingly, we found a similar bias in *vab-3(k109)* PD mutants, suggesting that the PD might have unique roles in these cells (Fig. 4). To uncover the function of the *vab-3*

A

Strain (n)	hlh-17::GFP expression pattern					
	on in DL/R	on in DL or DR	off in DL/R	on in VL/R	on in VL or VR	off in VL/R
Wild type (100)	99%	1%	0%	97%	3%	0%
vab-3(ns157) (104)	3%	43%	54%	44%	41%	15%
vab-3(ns157) + F14F3 (51)	73%	11%	16%	86%	9%	5%
vab-3(ns157) + vab-3 genomic locus (50)	60%	24%	16%	73%	20%	7%

B

Isoform A

sy281: G19R k143: G13Q ns157: S120N e648: W101opal k109: S75L e1796: I229T, L232H ju468: Q262amber

paired domain   homeodomain
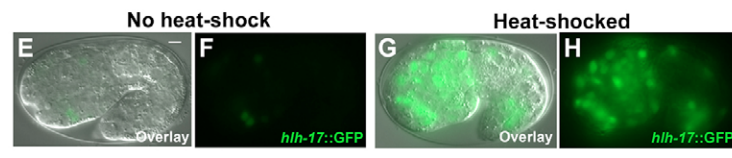
Isoform B — bx23

Isoform C

C

Paired Domain

```
human PAX7     : GQGRVNQLGGVFINGRPLPNHIRHKIVEMAHHGIRPCVISRQLRVSHGCVSKILCRYQETGSIRPGA
human PAX6     : SHSGVNQLGGVFVNGRPLPDSTRQKIVELAHSGARPCDISRILQVSNGCVSKILGRYYETGSIRPRA
zebrafish PAX7 : GQGRVNQLGGVFINGRPLPNHIRHKIVEMAHHGIRPCVISRQLRVSHGCVSKILCRYQETGSIRPGA
zebrafish PAX6 : SHSGVNQLGGVFVNGRPLPDSTRQKIVELAHSGARPCDISRILQVSNGCVSKILGRYYETGSIRPRA
VAB-3          : GHTGVNQLGGVFVNGRPLPDATRQRIVDLAHKGCRPCDISRLLQVSNGCVSKILCRYYESGTIRPRA

human PAX7     : IGGSKPRQVATPDVEKKIEEYKRENPGMFSWEIRDRLLKDGHCDRSTVPSG---LVSSISRVLRIKF
human PAX6     : IGGSKPR-VATPEVVSKIAQYKRECPSIFAWEIRDRLLSEGVCTNDNIPS-----VSSINRVLRNLA
zebrafish PAX7 : IGGSKPRQVATPDVEKRIEEYKRENPGMFSWEIRDKLLKDGVCDRGTVPSGEASSVSSISRVLRARF
zebrafish PAX6 : IGGSKPR-VATPEVVGKIAQYKRECPSIFAWEIRDRLLSEGVCTNDNIPS-----VSSINRVLRNLA
VAB-3          : IGGSKPR-VATSDVVEKIEDYKRDQPSIFAMEIRDKLLADNICNNETIPS-----VSSINRVLRNLA
```

Homeodomain

```
human PAX7     : RRSRTTFTAEQLEELEKAFERTHYPDIYTREELAQRTKLTEARVQVWFSNRRARWRKQA
human PAX6     : QRNRTSFTQEQIEALEKEFERTHYPDVFARERLAAKIDLPEARIQVWFSNRRAKWRREE
zebrafish PAX7 : RRSRTTFTAEQLEELEKEFERTHYPDIYTREELAQRTKLTEARVQVWFSNRRARWRKQA
zebrafish PAX6 : QRNRTSFTQEQIEALEKEFERTHYPDVFARERLAAKIDLPEARIQVWFSNRRAKWRREE
VAB-3          : QRNRTSFTQVQIESLEKEFERTHYPDVFARERLAQKIQLPEARIQVWFSNRRAKWRREE
```

D

	CEPsh			n
	VL	VR	DL/R	
Transgene	+	+	+	20
hlh-17::GFP expression	+	+	+	
Transgene	−	+	+	1
hlh-17::GFP expression	−	+	+	
Transgene	+	−	+	2
hlh-17::GFP expression	+	−	+	
Transgene	−	−	+	3
hlh-17::GFP expression	−	−	+	
Transgene	+	+	−	6
hlh-17::GFP expression	+	+	−	

No heat-shock

E Overlay **F** hlh-17::GFP

Heat-shocked

G Overlay **H** hlh-17::GFP

Fig. 6. *ns157* alters VAB-3, a Pax6/7-related protein.
(**A**) *vab-3(ns157)* rescue studies. Strains scored as in Fig. 4. VL/R and DL/R, ventral left/right and dorsal left/right CEPsh glia, respectively. *n*, number of animals. F14F3, *vab-3* cosmid. A representative line is shown for each construct. The *vab-3* genomic locus construct contains 24 kb surrounding and including the gene. (**B**) *C. elegans vab-3* gene structure. Boxes, exons; ∧-shaped lines, introns. Those exons marked with asterisks are specific for isoforms B and C. Paired domain and homeodomain in blue. *bx23* deletes isoform B exon 1. (**C**) Paired domain and homeodomain alignment of VAB-3 and indicated proteins. Pink, identical in all; blue, identical in all but one; gray, present in three of the proteins. (**D**) Mosaic analysis of *vab-3* control of *hlh-17*::expression. +/–, transgene/*hlh-17*::GFP expression present/absent; *n*, number of animals. (**E-H**) Induction of *hlh-17*::GFP reporter expression by overexpression of *vab-3* isoform A using a heat-inducible promoter. Merged DIC/fluorescence (E,G) and fluorescence (F,H) images of embryo without heat shock (E,F) and 90 minutes after heat shock (G,H).

HD, we examined reporter expression in *vab-3(e1796)* animals containing missense mutations in the VAB-3 HD (Fig. 6B). Although *hlh-17* expression was abrogated in both dorsal and ventral CEPsh glia in these animals, we found a surprising ventral bias in the failure to activate *ptr-10* expression (Fig. 4). Dorsal CEPsh glia expressing *ptr-10*::myrRFP but not *hlh-17*::GFP still possess normal posterior extensions ensheathing the nerve ring, consistent with our EM results (see Fig. S4 in the supplementary material).

These studies suggest two conclusions. First, different domains of VAB-3 may be important for controlling ventral and dorsal CEPsh glia differentiation, suggesting that the VAB-3 targets in

these cells might be different. Second, the differential perturbation of *ptr-10* and *hlh-17* expression in *vab-3*(*e1796*) animals suggests that *vab-3* regulates *hlh-17* and *ptr-10* expression independently.

### *hlh-17* cooperates with *vab-3* to regulate its own expression

To determine whether in addition to *mls-2* and *vab-3*, *hlh-17* also plays a role in CEPsh glia development, we used trimethylpsoralen mutagenesis to generate an *hlh-17* deletion, *ns204*, removing most of the bHLH domain (Materials and methods; see Fig. S5D in the supplementary material). *hlh-17*(*ns204*) mutants do not display obvious developmental defects or CEPsh glia abnormalities, as assessed by *hlh-17*::GFP and *ptr-10*::RFP expression, and AFD and AWC axons project normally in these mutants (see Fig. S6 in the supplementary material). Interestingly, however, whereas *hlh-17*::GFP expression in ventral CEPsh glia is normal in *hlh-17*(*ns204*) mutants, GFP expression levels are significantly reduced in *hlh-17*(*ns204*); *vab-3*(*ns157*) mutants (Table 1). We observed a similar result using a different *hlh-17* allele (*tm2850*; Table 1). We did not observe enhanced defects in *ptr-10*::RFP expression (see Fig. S7A,B in the supplementary material). These results suggest that *hlh-17* functions with *vab-3* to regulate its own expression.

hlh-17(*ns204*); *vab-3*(*ns157*) double mutants show no enhancement in axon guidance defects (92/204 defective AWC neurons, compare with Fig. 3I). We, therefore, wondered whether *hlh-17* might act redundantly with the *hlh-31* and *hlh-32* Olig-related genes to control axon guidance. To test this, we generated *hlh-32*(*ns223*) *hlh-17*(*ns204*) *hlh-31*(*ns217*) mutants by mutagenizing *hlh-17*(*ns204*) and then *hlh-17*(*ns204*) *hlh-31*(*ns217*) mutants with trimethylpsoralen (Materials and methods). The mutations we generated delete portions of the bHLH domains of each gene (see Fig. S5C in the supplementary material). Triple mutants are not defective in axon guidance, *hlh-17* or *ptr-10* expression, or dendrite extension, nor do they enhance the dendritic defects of *vab-3*(*ns157*) mutants (see Fig. S7 in the supplementary material). However, we found weak axon guidance defect enhancement in *hlh-32*(*ns223*) *hlh-17*(*ns204*) *hlh-31*(*ns217*); *vab-3*(*ns157*) mutants: whereas only 21/100 *vab-3*(*ns157*) animals in which ventral CEPsh glia expressed *hlh-17*::GFP had AWC axonal defects, 22/39 *hlh-32*(*ns223*) *hlh-17*(*ns204*) *hlh-31*(*ns217*); *vab-3*(*ns157*) mutants expressing *hlh-17*::GFP in ventral CEPsh glia had AWC axonal defects. Thus, *hlh-17* may function redundantly with *hlh-17*-related genes to regulate ventral CEPsh glia functions. However, since we could not detect expression of the *hlh-17*-related genes in CEPsh glia, it is also possible that they control axon guidance in other ways.

Finally, we note that a previous study suggested that the *hlh-17*(*ok487*) mutation promotes lethality (McMiller and Johnson, 2005). However, our extensive genetic studies of this mutation suggest that the lethality is not associated with the *hlh-17* lesion (data not shown). Furthermore, the *ok487* lesion is not a deletion, as previously reported, but an insertion of DNA into the *hlh-17* locus (see Fig. S5B in the supplementary material).

vab-3 but not *mls-2* is sufficient to promote *hlh-17* transcription

To determine whether *mls-2* and/or *vab-3* are sufficient to promote CEPsh gene transcription, we examined whether expression of heat-shock promoter::cDNA transgenes promoted ectopic *hlh-17*::GFP/*ptr-10*::myrRFP expression. We found that subjecting non-transgenic (*n*=160) or heat-shock promoter::*mls-2* embryos (*n*>100) to a 30-minute 34°C heat pulse failed to induce reporter expression.
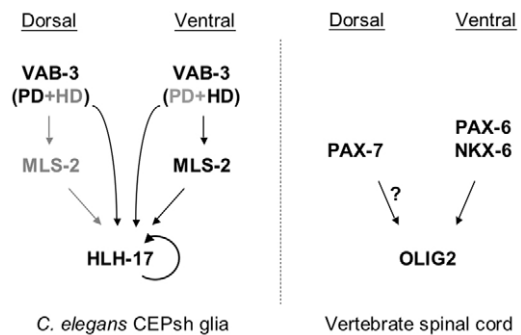
Fig. 7. Models for transcriptional control of ensheathing glia formation. In ventral *C. elegans* CEPsh glia and in ventral vertebrate spinal cords, Nkx family and Pax6-related proteins regulate Olig-related gene expression. In dorsal *C. elegans* CEPsh glia and in dorsal vertebrate spinal cords, a Pax7-related protein may promote Olig expression. Gray shading of the VAB-3 PD and HD reflects increased VAB-3 PD requirement in dorsal CEPsh glia for *hlh-17* expression. The homeodomain of VAB-3 is preferentially required in ventral glia for expression of *ptr-10*, suggesting a possible similar preference for *hlh-17*. In addition to regulation by VAB-3 and MLS-2, HLH-17 regulates its own expression.

Strikingly, however, *hlh-17*::GFP (and *ptr-10*::myrRFP, data not shown) was induced within 60 minutes of heat exposure throughout heat-shock promoter::*vab-3* embryos (Fig. 6E-H). Induction required a 500 bp *vab-3*-responsive element immediately upstream of the *hlh-17* translation start site (data not shown).

hlh-17::GFP induction was independent of *mls-2*, as *vab-3*-induced expression was still evident in *mls-2*(*ns156*) mutants (*n*=160, two lines examined). Furthermore, a heat-shock promoter::*vab-3* cDNA transgene was unable to induce ectopic expression of an *mls-2* promoter::GFP::*mls-2*::*mls-2* 3′ reporter (*n*=50, two lines observed). Thus, *vab-3* is sufficient to induce *hlh-17* expression. Furthermore, the rapid appearance of GFP suggests that *vab-3* might activate *hlh-17* directly.

Surprisingly, we found that *mls-2*::GFP expression in anterior cells was greatly reduced or absent in 200- to 350-minute *vab-3*(*ns157*) embryos (*n*>100), but was present at wild-type levels at later stages (*n*>50). VAB-3 protein (detected by antisera), however, was expressed in a grossly wild-type pattern in *mls-2*(*ns156*) mutants (data not shown). These results suggest that *vab-3* might also activate *hlh-17* via *mls-2*. Such feed-forward loops are common transcriptional motifs (Shen-Orr et al., 2002). Given the minor role of *mls-2* in regulating *hlh-17* expression in dorsal CEPsh glia, this alternative activation branch might be more important in ventral CEPsh glia (Fig. 7).

DISCUSSION
A transcriptional program promoting the development of ensheathing glia in *C. elegans*
The development of the vertebrate spinal cord has been extensively studied, and neuronal and glial transcriptional regulators within this structure have been described (Jessell, 2000; Rowitch, 2004; Nicolay et al., 2007). It has been unclear, however, whether similar transcriptional cascades control invertebrate glia development. The studies described here suggest similarities between *C. elegans* CEPsh glia and vertebrate oligodendrocytes. First, although myelin is not present in *C. elegans* (Ward et al., 1975; White et al., 1986), CEPsh glia, like oligodendrocytes, ensheath neuronal processes. Second, CEPsh and other *C. elegans* glia express HLH-17, the *C. elegans* protein most closely related to oligodendrocyte-expressed Olig2.

Table 1. *hlh-17* and *vab-3* together regulate *hlh-17*::GFP expression

Genotype*	Compared to[†]	Intensity of *hlh-17*::GFP			
		Higher	Same	Lower	n
Wild type[‡]	Wild type	12	20	9	41
hlh-17(ns204)	Wild type	9	28	4	41
hlh-17(tm2850)	Wild type	9	27	4	40
hlh-32(ns223) hlh-17(ns204) hlh-31(ns217)	Wild type	10	27	4	41
vab-3(ns157)	Wild type	4	28	13	45
vab-3(ns157)[§]	*vab-3(ns157)*	7	25	9	41
hlh-17(ns204); vab-3(ns157)	*vab-3(ns157)*	0	10	34	44
hlh-17(tm2850); vab-3(ns157)	*vab-3(ns157)*	0	7	34	41
hlh-32(ns223) hlh-17(ns204) hlh-31(ns217); vab-3(ns157)	*vab-3(ns157)*	0	4	36	40

*All animals also contained a genomically integrated *hlh-17*::GFP reporter transgene.
[†]Single animals of the indicated genotype were compared with either single wild-type or single *vab-3(ns157)* animals containing the same integrated *hlh-17*::GFP reporter transgene; relative fluorescence intensity levels were compared.
[‡]This comparison measures the variability of GFP expression within the *hlh-17*::GFP transgenic line in otherwise wild-type animals.
[§]This comparison measures the variability of GFP expression within the *hlh-17*::GFP transgenic line in *vab-3(ns157)* animals.

Third, although all four CEPsh glia express HLH-17 and ensheath neurons, cell lineages giving rise to dorsal and ventral CEPsh glia are unrelated, and these glia have distinct molecular signatures (Wadsworth et al., 1996), as is the case with oligodendrocytes in the ventral and dorsal regions of the vertebrate spinal cord. Fourth, here we show that HLH-17 expression is differentially regulated in dorsal and ventral CEPsh glia, reminiscent of the pattern of Olig2 expression in the vertebrate spinal cord (Fig. 7). HLH-17 expression in ventral CEPsh glia requires the MLS-2 and VAB-3 transcriptional regulators, whereas expression in dorsal CEPsh glia requires mainly VAB-3, and, specifically, the VAB-3 PD. MLS-2 is similar to Nkx superfamily proteins and is distantly related to Nkx6, which regulates ventral Olig2 expression in the neural tube. VAB-3 is the *C. elegans* protein most similar in sequence and domain structure to Pax6, which controls ventral Olig2 expression in vertebrate spinal cords (79% and 93% identity to the human PAX6 PD and HD, respectively), and to Pax7, which may regulate Olig2 expression in the dorsal spinal cord (71% and 65% identity to the PD and HD of human PAX7, respectively; Fig. 6C), although VAB-3 lacks an octapeptide sequence present in Pax7 (Jostes et al., 1990).

Interestingly, in *Pax6* mutant mice, oligodendrocyte precursor cell generation is delayed (Sun et al., 1998), suggesting that Pax6 might control Nkx6. We observed a similar relationship between VAB-3 and MLS-2, demonstrating that VAB-3 acts at early time points to control MLS-2 expression.

Together, our results hint at possible similarities between CEPsh glia development in *C. elegans* and the development of vertebrate oligodendrocytes; however, differences are also notable. Importantly, mice carrying *Olig2* mutations have fewer oligodendrocytes than wild-type animals (Zhou and Anderson, 2002), suggesting developmental roles for this gene. However, *hlh-17* mutations do not grossly perturb CEPsh glia generation or differentiation. One explanation for this may be redundancy: in vertebrates, *Olig2* and *Olig1* control oligodendrocyte numbers (Zhou and Anderson, 2002; Lu et al., 2002). We identified two proteins highly related to HLH-17, showing that triple *hlh* mutants display more penetrant axon guidance defects in a *vab-3* mutant background than *hlh-17* mutants alone. Although these defects could reflect redundancy in *C. elegans* Olig gene function, HLH-17 might also be redundant with other factors, or might primarily regulate CEPsh function post-developmentally. The persistence of *hlh-17* expression in CEPsh glia throughout adulthood is consistent with this possibility. *Olig2* and *Olig1* may function in controlling nervous system repair following injury (Ligon et al., 2006) and it is possible that HLH-17 and its relatives also have similar roles.

C. elegans CEPsh glia control neurite extension and guidance

We showed that ventral CEPsh glia play key roles in axon guidance, attributed at least in part to UNC-6/Netrin expression, which may function as a local cue to regulate guidance. These results might explain previous observations that the shapes of CEPsh glia and RIA neuron axons are correlated (Colón-Ramos et al., 2007). Short-range functions for Netrin-related proteins have been described (Baker et al., 2006), and Netrin is present on the periaxonal myelin of oligodendrocytes in the spinal cord, suggesting that it might serve local adhesive roles in these glia (Manitt et al., 2001).

The idea of UNC-6-directed local axon guidance raises the possibility that synaptogenesis defects recently reported in mutants lacking UNC-6 or its receptor, UNC-40 (Colón-Ramos et al., 2007), might not be due to direct roles in synapse formation, but to subtle neuronal guidance defects. Mosaic analysis, fluorescence imaging and gain-of-function experiments provided correlative evidence that ventral CEPsh glia influence the position of synapses between the AIY and RIA neurons. However, EM studies demonstrating that this correlation is not secondary to local axon positioning roles of CEPsh glia were not performed. Indeed, EM studies of wild-type animals show that ventral CEPsh glia are not apposed to AIY/RIA synapses; rather, glia contact the opposite side of the AIY axon from that where synapses occur. Furthermore, indirect extracellular glial access to these synapses is obstructed [(White et al., 1986); see supplementary fig. 1O of Colón-Ramos et al. (Colón-Ramos et al., 2007); Y.L. and S.S., unpublished], suggesting indirect roles for CEPsh glia in synaptogenesis. Definitive resolution of these issues awaits examination of AIY-RIA synapses in animals lacking CEPsh glia, and EM reconstructions of *unc-6*/*unc-40* mutants.

In addition to UNC-6, other axon guidance/branching proteins in the nerve ring are known, including SAX-3/Robo (Zallen et al., 1999), VAB-1/Eph (George et al., 1998; Zallen et al., 1999) and UNC-40/DCC (Chan et al., 1996). Whereas SAX-3 function in peripheral *C. elegans* neurons is regulated by SLT-1/Slit ligand, the nerve ring defects of *sax-3* mutants might reflect redundant interactions of SAX-3 with SLT-1 and a different ligand (Hao et al., 2001). *sax-3* defects include anteriorly displaced nerve rings and cell bodies, anterior axon projections, and defects in ventral projections and axon elongation (Zallen et al., 1999). Although most animals lacking ventral CEPsh glia show only axon guidance and branching defects, about 20% arrest development in the L1 stage, exhibiting anteriorly displaced nerve

rings and cell bodies (Fig. 3). It is possible, therefore, that CEPsh glia also secrete a SAX-3/Robo ligand regulating nerve ring positioning, assembly and axon guidance. The weak penetrance of the *sax-3*-like defects we observed might reflect our inability to ablate all four CEPsh glia simultaneously.

A unique genetic system for studying glia in vivo

A major obstacle to studying glia and their interactions with neurons has been their trophic support of neurons. Manipulation of glia, in vivo or in vitro, often leads to the death of associated neurons, precluding detailed studies of glial effects on other neuronal functions. One approach to circumvent this difficulty has been to culture neurons with survival factors, examining the consequences of glia re-addition. This approach uncovered roles for glia-secreted cholesterol in neuronal activity (Mauch et al., 2001) and for glia-produced thrombospondin in synapse formation (Christopherson et al., 2005). However, in vivo verification of these studies remains challenging.

Our studies reveal that the *C. elegans* CEPsh glia, while possessing morphological, functional and molecular similarities to vertebrate glia, differ from their vertebrate counterparts in that they are not required for neuronal survival. This observation has allowed us to explore glial function in vivo and to demonstrate key roles for these cells in dendrite and axon extension. Our results suggest that *C. elegans* might, therefore, be useful for identifying glial contributions to the development and function of all nervous systems.

Supplementary material
Supplementary material for this article is available at
http://dev.biologists.org/cgi/content/full/135/13/2263/DC1

References

Adler, C. E., Fetter, R. D. and Bargmann, C. I. (2006). UNC-6/Netrin induces neuronal asymmetry and defines the site of axon formation. *Nat. Neurosci.* **9**, 511-518.

Altschul, S. F., Gish, W., Miller, W., Myers, E. W. and Lipman, D. J. (1990). Basic local alignment search tool. *J. Mol. Biol.* **215**, 403-410.

Baker, K. A., Moore, S. W., Jarjour, A. A. and Kennedy, T. E. (2006). When a diffusible axon guidance cue stops diffusing: roles for netrins in adhesion and morphogenesis. *Curr. Opin. Neurobiol.* **16**, 529-534.

Bao, Z., Murray, J. I., Boyle, T., Ooi, S. L., Sandel, M. J. and Waterston, R. H. (2006). Automated cell lineage tracing in *Caenorhabditis elegans*. *Proc. Natl. Acad. Sci. USA* **103**, 2707-2712.

Bargmann, C. I. and Avery, L. (1995). Laser killing of cells in *Caenorhabditis elegans*. *Methods Cell Biol.* **48**, 225-250.

Brenner, S. (1974). The genetics of *Caenorhabditis elegans*. *Genetics* **77**, 71-94.

Briscoe, J., Pierani, A., Jessell, T. M. and Ericson, J. (2000). A homeodomain protein code specifies progenitor cell identity and neuronal fate in the ventral neural tube. *Cell* **101**, 435-445.

Cai, J., Qi, Y., Hu, X., Tan, M., Liu, Z., Zhang, J., Li, Q., Sander, M. and Qiu, M. (2005). Generation of oligodendrocyte precursor cells from mouse dorsal spinal cord independent of Nkx6 regulation and Shh signaling. *Neuron* **45**, 41-53.

Chan, S. S., Zheng, H., Su, M. W., Wilk, R., Killeen, M. T., Hedgecock, E. M. and Culotti, J. G. (1996). UNC-40, a C. elegans homolog of DCC (Deleted in Colorectal Cancer) is required in motile cells responding to UNC-6 netrin cues. *Cell* **87**, 187-195.

Chisholm, A. D. and Horvitz, H. R. (1995). Patterning of the *Caenorhabditis elegans* head region by the Pax-6 family member *vab-3*. *Nature* **377**, 52-55.

Christopherson, K. S., Ullian, E. M., Stokes, C. C., Mullowney, C. E., Hell, J. W., Agah, A., Lawler, J., Mosher, D. F., Bornstein, P. and Barres, B. A. (2005). Thrombospondins are astrocyte-secreted proteins that promote CNS synaptogenesis. *Cell* **120**, 421-433.

Cinar, H. N. and Chisholm, A. D. (2004). Genetic analysis of the *Caenorhabditis elegans pax-6* locus: roles of paired domain-containing and nonpaired domain-containing isoforms. *Genetics* **168**, 1307-1322.

Colón-Ramos, D. A., Margeta, M. A. and Shen, K. (2007). Glia promote local synaptogenesis through UNC-6(netrin) signaling in C. elegans. *Science* **318**, 103-106.

Edmondson, J. C., Liem, R. K., Kuster, J. E. and Hatten, M. E. (1988). Astrotactin: a novel neuronal cell surface antigen that mediates neuron-astroglial interactions in cerebellar microcultures. *J. Cell Biol.* **106**, 505-517.

Fire, A., Harrison, S. W. and Dixon, D. (1990). A modular set of *lacZ* fusion vectors for studying gene expression in *Caenorhabditis elegans*. *Gene* **93**, 189-198.

Fishell, G. and Hatten, M. E. (1991). Astrotactin provides a receptor system for CNS neuronal migration. *Development* **113**, 755-765.

Fogarty, M., Richardson, W. D. and Kessaris, N. (2005). A subset of oligodendrocytes generated from radial glia in the dorsal spinal cord. *Development* **132**, 1951-1959.

Fukushige, T., Hawkins, M. G. and McGhee, J. D. (1998). The GATA-factor *elt-2* is essential for formation of the *Caenorhabditis elegans* intestine. *Dev. Biol.* **198**, 286-302.

George, S. E., Simokat, K., Hardin, J. and Chisholm, A. D. (1998). The VAB-1 Eph receptor tyrosine kinase functions in neural and epithelial morphogenesis in C. elegans. *Cell* **92**, 633-643.

Hao, J. C., Yu, T., Fujisawa, K., Culotti, J. G., Gengyo-Ando, K., Mitani, S., Moulder, G., Barstead, R., Tessier-Lavigne, M. and Bargmann, C. (2001). C. elegans slit acts in midline, dorsal-ventral, and anterior-posterior guidance via the SAX-3/Robo receptor. *Neuron* **32**, 25-38.

Heiman, M. G. and Shaham, S. (2007). Ancestral roles of glia suggested by the nervous system of *Caenorhabditis elegans*. *Neuron Glia Biol.* **3**, 55-61.

Hosoya, T., Takizawa, K., Nitta, K. and Hotta, Y. (1995). glial cells missing: a binary switch between neuronal and glial determination in Drosophila. *Cell* **82**, 1025-1036.

Huang, L. S., Tzou, P. and Sternberg, P. W. (1994). The *lin-15* locus encodes two negative regulators of *Caenorhabditis elegans* vulval development. *Mol. Biol. Cell* **5**, 395-411.

Jessell, T. M. (2000). Neuronal specification in the spinal cord: inductive signals and transcriptional codes. *Nat. Rev. Genet.* **1**, 20-29.

Jiang, Y., Horner, V. and Liu, J. (2005). The HMX homeodomain protein MLS-2 regulates cleavage orientation, cell proliferation and cell fate specification in the C. elegans postembryonic mesoderm. *Development* **132**, 4119-4130.

Jones, B. W., Fetter, R. D., Tear, G. and Goodman, C. S. (1995). glial cells missing: a genetic switch that controls glial versus neuronal fate. *Cell* **82**, 1013-1023.

Jostes, B., Walther, C. and Gruss, P. (1990). The murine paired box gene, Pax7, is expressed specifically during the development of the nervous and muscular system. *Mech. Dev.* **33**, 27-37.

Kidd, T., Bland, K. S. and Goodman, C. S. (1999). Slit is the midline repellent for the robo receptor in Drosophila. *Cell* **96**, 785-794.

Krause, M. and Hirsh, D. (1987). A trans-spliced leader sequence on actin mRNA in C. elegans. *Cell* **49**, 753-761.

Kuwabara, P. E. and Labouesse, M. (2002). The sterol-sensing domain: multiple families, a unique role? *Trends Genet.* **18**, 193-201.

Kuwabara, P. E., Lee, M. H., Schedl, T. and Jefferis, G. S. (2000). A C. elegans patched gene, *ptc-1*, functions in germ-line cytokinesis. *Genes Dev.* **14**, 1933-1944.

L'Etoile, N. D. and Bargmann, C. I. (2000). Olfaction and odor discrimination are mediated by the C. elegans guanylyl cyclase ODR-1. *Neuron* **25**, 575-586.

Ligon, K. L., Fancy, S. P., Franklin, R. J. and Rowitch, D. H. (2006). Olig gene function in CNS development and disease. *Glia* **54**, 1-10.

Liu, R., Cai, J., Hu, X., Tan, M., Qi, Y., German, M., Rubenstein, J., Sander, M. and Qiu, M. (2003). Region-specific and stage-dependent regulation of Olig gene expression and oligodendrogenesis by Nkx6.1 homeodomain transcription factor. *Development* **130**, 6221-6231.

Lu, Q. R., Yuk, D., Alberta, J. A., Zhu, Z., Pawlitzky, I., Chan, J., McMahon, A. P., Stiles, C. D. and Rowitch, D. H. (2000). Sonic hedgehog-regulated oligodendrocyte lineage genes encoding bHLH proteins in the mammalian central nervous system. *Neuron* **25**, 317-329.

Lu, Q. R., Sun, T., Zhu, Z., Ma, N., Garcia, M., Stiles, C. D. and Rowitch, D. H. (2002). Common developmental requirement for Olig function indicates a motor neuron/oligodendrocyte connection. *Cell* **109**, 75-86.

Maduro, M. and Pilgrim, D. (1995). Identification and cloning of *unc-119*, a gene expressed in the *Caenorhabditis elegans* nervous system. *Genetics* **141**, 977-988.

Manitt, C., Colicos, M. A., Thompson, K. M., Rouselle, E., Peterson, A. C. and Kennedy, T. E. (2001). Widespread expression of netrin-1 by neurons and oligodendrocytes in the adult mammalian spinal cord. *J. Neurosci.* **21**, 3911-3922.

Mauch, D. H., Nagler, K., Schumacher, S., Goritz, C., Muller, E. C., Otto, A. and Pfrieger, F. W. (2001). CNS synaptogenesis promoted by glia-derived cholesterol. *Science* **294**, 1354-1357.

McMiller, T. L. and Johnson, C. M. (2005). Molecular characterization of HLH-17, a C. elegans bHLH protein required for normal larval development. *Gene* **356**, 1-10.

Mello, C. and Fire, A. (1995). DNA transformation. *Methods Cell Biol.* **48**, 451-482.

Mello, C. C., Kramer, J. M., Stinchcomb, D. and Ambros, V. (1991). Efficient gene transfer in *C. elegans*: extrachromosomal maintenance and integration of transforming sequences. *EMBO J.* **10**, 3959-3970.

Meyer-Franke, A., Kaplan, M. R., Pfrieger, F. W. and Barres, B. A. (1995). Characterization of the signaling interactions that promote the survival and growth of developing retinal ganglion cells in culture. *Neuron* **15**, 805-819.

Miller, D. M., 3rd, Desai, N. S., Hardin, D. C., Piston, D. W., Patterson, G. H., Fleenor, J., Xu, S. and Fire, A. (1999). Two-color GFP expression system for *C. elegans*. *Biotechniques* **26**, 914-918.

Nass, R., Hahn, M. K., Jessen, T., McDonald, P. W., Carvelli, L. and Blakely, R. D. (2005). A genetic screen in *Caenorhabditis elegans* for dopamine neuron insensitivity to 6-hydroxydopamine identifies dopamine transporter mutants impacting transporter biosynthesis and trafficking. *J. Neurochem.* **94**, 774-785.

Nicolay, D. J., Doucette, J. R. and Nazarali, A. J. (2007). Transcriptional control of oligodendrogenesis. *Glia* **55**, 1287-1299.

Noctor, S. C., Flint, A. C., Weissman, T. A., Dammerman, R. S. and Kriegstein, A. R. (2001). Neurons derived from radial glial cells establish radial units in neocortex. *Nature* **409**, 714-720.

Novitch, B. G., Chen, A. I. and Jessell, T. M. (2001). Coordinate regulation of motor neuron subtype identity and pan-neuronal properties by the bHLH repressor Olig2. *Neuron* **31**, 773-789.

Perens, E. A. and Shaham, S. (2005). *C. elegans daf-6* encodes a patched-related protein required for lumen formation. *Dev. Cell* **8**, 893-906.

Rowitch, D. H. (2004). Glial specification in the vertebrate neural tube. *Nat. Rev. Neurosci.* **5**, 409-419.

Sagasti, A., Hobert, O., Troemel, E. R., Ruvkun, G. and Bargmann, C. I. (1999). Alternative olfactory neuron fates are specified by the LIM homeobox gene *lim-4*. *Genes Dev.* **13**, 1794-1806.

Satterlee, J. S., Sasakura, H., Kuhara, A., Berkeley, M., Mori, I. and Sengupta, P. (2001). Specification of thermosensory neuron fate in *C. elegans* requires *ttx-1*, a homolog of Otd/Otx. *Neuron* **31**, 943-956.

Serafini, T., Colamarino, S. A., Leonardo, E. D., Wang, H., Beddington, R., Skarnes, W. C. and Tessier-Lavigne, M. (1996). Netrin-1 is required for commissural axon guidance in the developing vertebrate nervous system. *Cell* **87**, 1001-1014.

Shaham, S. (2006). Glia-neuron interactions in the nervous system of *C. elegans*. *Curr. Opin. Neurobiol.* **16**, 522-528.

Shen-Orr, S. S., Milo, R., Mangan, S. and Alon, U. (2002). Network motifs in the transcriptional regulation network of *Escherichia coli*. *Nat. Genet.* **31**, 64-68.

Sulston, J. E. and Hodgkin, J. (1988). Methods. In *The Nematode Caenorhabditis elegans* (ed. W. B. Wood), pp. 587-606. Cold Spring Harbor: Cold Spring Harbor Laboratory Press.

Sulston, J. E., Schierenberg, E., White, J. G. and Thomson, J. N. (1983). The embryonic cell lineage of the nematode *Caenorhabditis elegans*. *Dev. Biol.* **100**, 64-119.

Sun, T., Pringle, N. P., Hardy, A. P., Richardson, W. D. and Smith, H. K. (1998). Pax6 influences the time and site of origin of glial precursors in the ventral neural tube. *Mol. Cell. Neurosci.* **12**, 228-239.

Takebayashi, H., Nabeshima, Y., Yoshida, S., Chisaka, O., Ikenaka, K. and Nabeshima, Y. (2002). The basic helix-loop-helix factor Olig2 is essential for the development of motoneuron and oligodendrocyte lineages. *Curr. Biol.* **12**, 1157-1163.

Vallstedt, A., Muhr, J., Pattyn, A., Pierani, A., Mendelsohn, M., Sander, M., Jessell, T. M. and Ericson, J. (2001). Different levels of repressor activity assign redundant and specific roles to Nkx6 genes in motor neuron and interneuron specification. *Neuron* **31**, 743-755.

Vallstedt, A., Klos, J. M. and Ericson, J. (2005). Multiple dorsoventral origins of oligodendrocyte generation in the spinal cord and hindbrain. *Neuron* **45**, 55-67.

Wadsworth, W. G., Bhatt, H. and Hedgecock, E. M. (1996). Neuroglia and pioneer neurons express UNC-6 to provide global and local netrin cues for guiding migrations in C. elegans. *Neuron* **16**, 35-46.

Wang, W., Lo, P., Frasch, M. and Lufkin, T. (2000). Hmx: an evolutionary conserved homeobox gene family expressed in the developing nervous system in mice and *Drosophila*. *Mech. Dev.* **99**, 123-137.

Ward, S., Thomson, N., White, J. G. and Brenner, S. (1975). Electron microscopical reconstruction of the anterior sensory anatomy of the nematode *Caenorhabditis elegans*. *J. Comp. Neurol.* **160**, 313-337.

White, J. G., Southgate, E., Thomson, J. N. and Brenner, S. (1986). The structure of the nervous system of the nematode *Caenorhabditis elegans*. *Philos. Trans. R. Soc. Lond. B Biol. Sci.* **314**, 1-340.

Wicks, S. R., Yeh, R. T., Gish, W. R., Waterston, R. H. and Plasterk, R. H. (2001). Rapid gene mapping in *Caenorhabditis elegans* using a high density polymorphism map. *Nat. Genet.* **28**, 160-164.

Yandell, M. D., Edgar, L. G. and Wood, W. B. (1994). Trimethylpsoralen induces small deletion mutations in *Caenorhabditis elegans*. *Proc. Natl. Acad. Sci. USA* **91**, 1381-1385.

Zallen, J. A., Kirch, S. A. and Bargmann, C. I. (1999). Genes required for axon pathfinding and extension in the *C. elegans* nerve ring. *Development* **126**, 3679-3692.

Zhou, Q. and Anderson, D. J. (2002). The bHLH transcription factors OLIG2 and OLIG1 couple neuronal and glial subtype specification. *Cell* **109**, 61-73.

Zhou, Q., Wang, S. and Anderson, D. J. (2000). Identification of a novel family of oligodendrocyte lineage-specific basic helix-loop-helix transcription factors. *Neuron* **25**, 331-343.